


Article

High Photocurrent Density and Continuous Electron Emission Characterization of a Multi-Alkali Antimonide Photocathode

Jun Dai ¹, Yikun Ding ¹, Cunjun Ruan ^{1,2,*} , Xiangyan Xu ^{3,*} and Hulin Liu ³

¹ School of Electronic and Information Engineering, Beihang University, Beijing 100191, China; eedaijun@buaa.edu.cn (J.D.); dingyikun@buaa.edu.cn (Y.D.)

² Beijing Key Laboratory for Microwave Sensing and Security Applications, Beihang University, Beijing 100191, China

³ Xi'an Institute of Optics and Precision Mechanics, Chinese Academy of Sciences, Xi'an 710119, China; haozian_cn@163.com

* Correspondence: ruancunjun@buaa.edu.cn (C.R.); xuxy@opt.ac.cn (X.X.)

Received: 27 October 2020; Accepted: 17 November 2020; Published: 24 November 2020



Abstract: High photocurrent density cathodes that enable small cross-section electron beams are required for high-power terahertz vacuum devices. Multi-alkali antimonide photocathodes may be well suited for generating sub-mm electron beam sources. This paper involves the repeatability, stability, uniformity, and linearity experiments of the multi-alkali antimonide photocathodes electron emission operations under a continuous-wave 450 nm laser with a bias voltage of 5000 V. The effect of heat, electric contact, and cathode surface roughness to emission characterizations is analyzed. The methods to maintain the high-current-density emission and avoid the fatigue of the photocathode are verified. The emission can be repeated with increased optical power. The stable photocurrent density of near 1 A/cm² and maximum current density of near 1.43 A/cm² is recorded. The continuous photocurrent density is significantly improved compared to the current density reported in traditional applications. It is found that the current curves measuring at different areas of the photocathode differ greatly after the laser power of 800 mW. The increase in current for some areas may be attributed to the conductive current caused by built-in electric fields between the emission rough area and its adjacent areas.

Keywords: continuous high current density emission; nonuniformity emission; nonlinear emission; built-in electric field

1. Introduction

Vacuum electronic devices are widely used in microwave and terahertz (THz) practical applications, as they can provide efficient high-power electromagnetic output [1]. As vacuum devices evolved from MHz to THz, high current electron beams with sub-mm cross-sections are required due to the physics mechanisms of frequency and geometry correlation. The development of THz power chips, including THz vacuum photodiodes that could translate optical source to THz band and THz vacuum amplifiers that could amplify THz signals, have motivated us to develop high current density cathodes with ultra-small size [2]. In addition, emerging research in high power THz radiation source based on planar antenna integrated vacuum photodiode also requires high current density electron emission source [3,4].

Multi-alkali antimonide photocathode has been considered to be the strongest candidate for a high-brightness electron source. It has a comparatively shorter response time (approximately hundreds of femtoseconds) and can be operated with quantum efficiency above 15% over a wide spectral range, which enables both high frequency and high current density operations for THz vacuum devices

and radiation sources [5]. The methods to develop the multi-alkali antimonide photocathode has been extensively researched and reviewed over the past decades [6–8]. The fabrication technique to achieve a high-quantum-efficiency multi-alkali antimonide photocathode has followed a similar and empirical process [9]. The photocathode growth process in this paper also using the process only with some difference in the vacuum pressure, temperature, and evaporation control. Although the physics of the process is far from clear, much progress has been achieved through experiments for photocathodes applying in a wide range of applications in the detectors and electron guns [10]. As a detecting material, photocathodes are mainly used in either continuous mode or pulse mode under weak illumination [11]. In most of the detecting applications, the photocathodes are designed to operate below $1 \mu\text{A}/\text{cm}^2$, which is a very low current density [12]. When used as an electron gun material, photocathodes are mainly used in short pulse or ultrashort pulse mode because continuous emission is always difficult and costly [13]. However, in traditional applications, the spectrum sensitivity and quantum efficiency are emphasized [14]. Little attention has been focused on the applications that require the high-repetition-rate emission or continuous emission at a high current density, which often results in fatigue of the photocathode.

Sommer has pointed out that the stability of the photocurrent at a higher absolute value will be affected by the ion bombardment [15]. It has been revealed that the heat emanating may raise the temperature of the photocathode, leading to a possible loss in the output current [4]. Simulations show that the local heating problem can be solved using a more thermally conductive substrate, such as a diamond [16]. Poor electric contact designs will cause electrolytic decomposition of the photocathode [17]. A previous study on high brightness emission has shown that a strong electric field is needed to overcome the big emittance caused by the surface roughness of the photocathode [18]. For high current density emissions in THz applications, the uniformity and linearity caused by the surface roughness are also significant to avoid the fluctuation in THz current.

This study aims to explore the repeatability, stability, uniformity, and linearity of the alkali antimonide photocathode with small areas operating at high current density in CW mode through experiments. The effect and tolerance of the photocathode growth process are also studied. The photocathode growth technology was optimized to support the operations at high current density following the suggestions to avoid cathode damage and promote quantum efficiency [16]. The performances of the photocathode were characterized by measuring the anode current as a function of laser power. The continuous emission performances of the photocathodes in different areas were measured and discussed. The new findings of the nonlinear emission characterization are analyzed theoretically.

2. Materials and Experimental Details

Traditional technology to fabricate multi-alkalis antimonide photocathode usually relies on a sequential growth of Potassium (K), Antimony (Sb), Sodium (Na), and Cesium (Cs) under ultra-high vacuum conditions. To support high current density emission operations, we made two changes to the traditional photocathode growth technology. First, a diamond wafer is utilized as the cathode substrate due to its high thermal conductivity. As there are great difficulties in sealing the diamond substrate with a metal tube body, we simply put a polycrystal diamond substrate inner the tube body by connecting it with a metal holder, as shown in Figure 1. Second, an aluminum (Al) film was coated on the diamond to provide electric contact. The primary technical indicators for the THz devices listed in the introduction are the current density generated in a small area, which is indicated to be from $3 \mu\text{m} \times 3 \mu\text{m}$ to $300 \mu\text{m} \times 300 \mu\text{m}$ [2]. We also want to reduce the strict requirements of the photocathode growth process, for example, the global uniformity and small surface roughness. A photocathode with bad surface consistency is supposed to be explored. So, the photocathode chemical elements are designed to evaporate in a horizontal direction. The chemical elements in the traditional chemical vapor growth process deposit in the vertical direction of the ground plane. This fabrication setup may enhance the cathode surface roughness in the fringe areas of the substrate wafer, as well as uniformity difference.

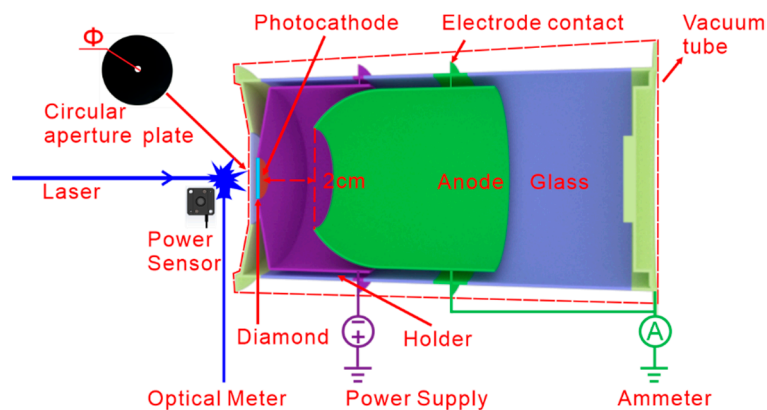


Figure 1. Schematic diagram of the electron emission experiment setup.

During the fabrication of the photocathode, the photocathode and the collecting anode are always connected to form a path with the micro-current meter and high-temperature wire. A tungsten lamp as a stable light source is placed outside the photocathode table and shines on the photocathode through a window. The tungsten lamp current is maintained unchanged during the process to make sure the light intensity is constant. The extracted photocurrent generated by the photocathode represents the sensitivity characteristics of the photocathode, and the manufacturing process of the cathode is then adjusted and controlled according to the change of the photocurrent to achieve the optimized photocathode fabrication and highest emission current.

At the beginning of the fabrication procedures, the alkali and Antimony metals went through a degassing process. Then, the tube was evacuated to 1.0×10^{-6} Pa. The temperature of the fabrication chamber was set to near 200 °C. The evaporation begins with the K process. K evaporation was performed with control through the feedback from the photocurrent of the cathode composition film. K source can be shut down temporarily until the maximum of extracted current was achieved. The following Sb source was evaporated with the same process control. Then, K and Sb were alternately deposited until the photocurrent reaches the peak to establish a K-Sb film. The Na process needs the current to be increased to its extremum point and then decreased to half of the peak current. Then, K and Sb were alternately deposited once again with current monitoring to form a transparent Na_2KSb film through chemical reactions.

Theoretical analysis has shown that the interface between the p-type Na_2KSb film and n-type cesium antimonide compound can bring down the electron affinity below the bottom of the conduction band of Na_2KSb . The drift field that arises at the heterointerface enables almost all the photogenerated electrons within the cathode to reach the surface [19]. To enhance the emission current through the multilayer structure growth, considerations must be taken to adjust the evaporation and doping concentrations on both p-type and n-type compound. Therefore, the correct doping of Cs and Sb is essential for the growth of the dipole layer. To perform the growth, the temperature was optimized to 160 °C. Then, the alternating evaporations of Cs and Sb over the transparent Na_2KSb film was used. The whole fabrication was completed with the roasting process to eliminate the redundant alkali metals. Finally, a transmission-type multi-alkalis antimonide photocathode was deposited on a 0.3 mm thick diamond substrate in a vacuum tube assembly. The vacuum diode tube, marked with a dotted line in Figure 1, was applied for the measurement of emission performance. The photocathode film was kept parallel to the optical glass window at a distance of 1 mm and mounted on an electric holder. The anode was aligned coaxially to the photocathode surface. The distance between the photocathode and its nearest anode area is 2 cm.

The experimental setup for the electron emission test consists of a photocathode vacuum tube, a circular aperture plate, a Thorlabs PM100 power meter console, an energy measurement sensor, quartz lenses, and power supply, as illustrated in Figure 1. A continuous-wave blue laser with a

wavelength of 450 nm was used for excitation of the photocathode. Quartz lenses and circular aperture plates are used for enhancing the input optical intensity and aligning visible light beam to the center of the photocathode illumination areas. The emission areas are all circular with a diameter of $\Phi = 0.5$ mm. It is bigger than $300\text{ }\mu\text{m} \times 300\text{ }\mu\text{m}$ which is enough for the requirement of the applications. Laser powers were all measured near the window of the vacuum tube using Thorlabs S405 power sensor whose maximum detecting power is 5 W. The actual incident laser power to the glass was about half of the measured power. The diameter of the laser beam is bigger than the diameter of the circular aperture, which causes half of the power to be blocked by the plate. The power illuminated at the photocathode is proportional to the measured power, yet it is less than half of the measured power. The direct current power supply was used to provide a biased voltage between photocathode and anode at 5000 V. The value of the collected anode current will be monitored using a passive QILIGANG B5C1 ammeter with an accuracy of 0.01 mA, which is made by Chanan Group Co. Ltd. (Guangzhou, China).

3. Results and Discussion

3.1. Repeatability and Stability

As mentioned in the introduction, for high-repetition-rate emission or continuous emission, the thermal storage may be the main reason for the deterioration of the photocathode because it leads to the decomposition of the surface compound. The thermal storage comes from the joule heat, carrier recombination heat, and optical absorption heat accumulation. Before using diamond as substrate material, we have fabricated four tubes using a borosilicate glass substrate whose thermal conductivity is about $1.3\text{ W/m}\cdot\text{K}$. The glass substrate serves as the optical window of the testing tubes as well. The best stable current density from limit tests we got was beyond 30 mA/cm^2 at 1500 V. When we further increased the incident power of CW laser illumination, the current of the cathode tube rapidly reached its plateau and then descended fleetly. During one of the limit tests, the glass substrate began to crack as the current reached its peak. Therefore, the thermal storage may affect the repeatability and stability of the emission photocurrent when operating at high-repetition-rate emission or continuous emission mode, which will lead to accuracy problems in generating THz signal and radiation.

The repeatability experiments with three seconds of exposure time are carried out at a randomly chosen linear area near the center of the diamond wafer. The bias voltage of the testing vacuum diode tube is maintained to be 5000 V during the experiments. No current drift was observed during the exposure. The mean photocurrent line of three current lines measured at different power is shown in Figure 2. The only error happens at 800 mW, 1200 mW, and 1400 mW shows the standard deviation is under 2.9%, which indicates the high repeatability of the emission current. The maximum current density measure at 1.8 mA near 1 A/cm^2 , was recorded as stable.

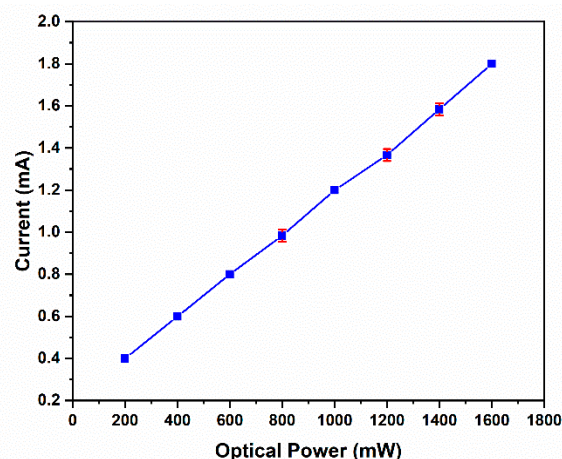


Figure 2. Plots of the current measured at different laser powers.

To find out the heat tolerance of the photocathode using a diamond substrate, stability experiments of electron emission with the optical power at 1600 mW were carried out. As we can see from Figure 3., high continuous emission current density at near 1 A/cm² could be maintained after the current drop. The current drop usually happened in the time slot of 20–30 min after the beginning of the experiments. The decay performance of the photocathode is common among the different photocathodes with different measurement environments [2,12]. At beginning of the test, the photocathode will undergo a process of a sharp temperature increase. A bad thermal conductivity of the substrate leads to a long time to reach a balance between heat accumulation and dissipation. The drop at different times in the two measurements can be attributed to instabilities in the laser source. The loss of the performance in the vacuum of 1.0×10^{-6} Pa is mainly due to the Cs desorption from the surface. The observed current decay suggested that the diamond substrate in the tube doesn't dissipate the heat effectively. The reason is that the interior of the testing tube is a vacuum where heat is conducted very slowly. Besides, the substrate is held by a Kovar alloy structure. Though the diamond has thermal conductivity near 2000 W/m·K, the thermal conductivity of Kovar alloy is near 50 W/m·K, which makes it difficult to spread the heat from inside to the outside of the tube very soon. If the diamond substrate is also used as an optical window, the situation could be much better. The heat can be conducted faster, and other cooling technologies are convenient to be applied. So, the technique of the sealing-in between diamond and metal must be tackled in the future.

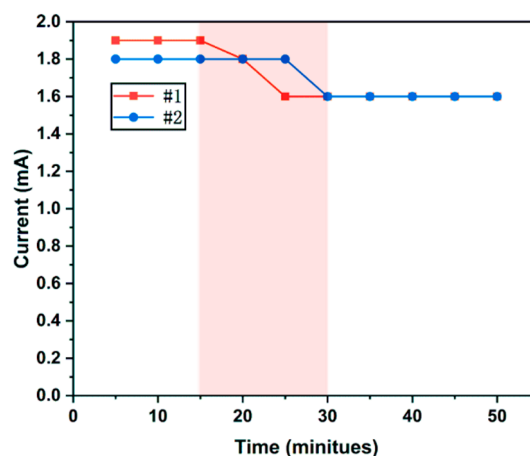


Figure 3. Plots of the current measured at 1600 mW with a five-minute interval.

3.2. Uniformity and Linearity

The uniformity and linearity measurements of the photocathode film are performed extensively in different areas. Figure 4. shows the selected continuous emission characterization from the typical areas. The marked areas in the circle on the left of Figure 4 represent their adjacent areas. The red line shows that the maximum current density is 1.43 A/cm² (at 2.8 mA), which is close to the current density reported with Cs₃Sb photocathode [12]. When the optical power is below 300 mW, it is not obvious to see the emission difference between different areas. The emission current measured between different areas with the optical power below 100 mW shows a difference below 8%, which indicates that the non-uniformity of the photocathode won't be a big problem when the photocathode is operated under weak illumination. It can be seen that the emission current performances are very different especially when the laser power is above 800 mW. This non-uniformity at high current emission from different areas may be caused by fabrication technology. Generally, the sequential deposition to fabricate the multi-alkalis antimonide photocathode is an unreliable process because the chemical reaction during the cathode growth is very sensitive to many parameters such as temperature, pressure, and deposition rates [9]. Any little change in the parameters could affect the homogeneity of the cathode chemical compositions and surface states. In our cathode growth setup, the evaporation directions of all the

multi-alkalis and antimonide metal sources are difficult to confine. The non-uniformity behaviors are also the results of the intentional design in the fabrication setup.

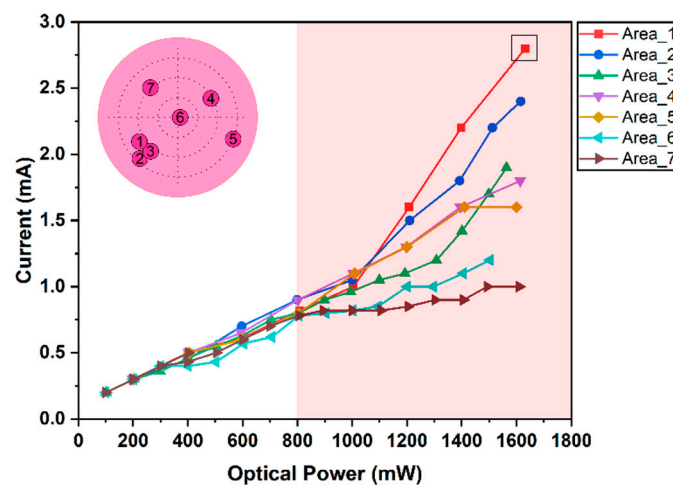


Figure 4. Plots of the current monitored at different laser powers and different areas.

It should be noted that the current characteristics in Area_1, Area_2, and Area_3 are exhibiting a current enhancement while Area_6 and Area_7 are exhibiting a saturation-like behavior at higher optical power. Area_1, Area_2, and Area_3 almost locate at the same place. The currents measured at these areas also indicate the repeatability of nonlinear emission. Area_4 and Area_5 both exhibit linear behavior. Actually, Area_4 and Area_5 also represent most of the emission areas. The emission scheme for different areas photocathode is the same. The unique difference is the uniformity of the cathode related to the whole processing and treatment. It is easy to understand the emission current rises linearly for most of the areas when the light power increases in the condition of the constant anode voltage. With more photon incident to the photocathode, the emission current is consequently elevated. It is also reasonable that some central areas, for example, Area_6, show a loss of output linearity owing to the effect of heat accumulation. The fatigue of the cathode is due to the frequent measurements in the above repeatability and stability experiments. Area_7 also represents a random area with a big sheet resistance caused by cathode nonuniformity.

It is interesting to see the current lines of some areas are beyond the linear lines after 800 mW. The current increase effect has also been observed in the photomultiplier tubes. The reasons are usually complicated and can be categorized as follows: thermionic emission current, field emission current, ionization current from gases. Thermionic emission current is a typical kind of dark current. It is difficult to generate mA level dark current within such a small area. The field between the cathode and anode is about 2500 V/cm. This is very low compared to the threshold of the field emission. Ionization current from gases is a serious problem for pulse operations because a large current is produced when the positive ions strike the photocathode. If there is an ionization current, the increase of the current could exist in any emission areas. At least, it will occur at the emission zones with the same radius. The experiments don't approve of all these kinds of effects. Also, in our previous experiments, we have measured the performance of the photocathode on Sapphire regarding the variation of laser spot size as a function of laser power using the same laser. The linear results help eliminate other unknown effects from the laser source [20].

The cathode fabrication and testing can only be performed in the ultrahigh vacuum environment ($\sim 10^{-6}$ Pa). The presence of air will lead to the oxidation of the photocathode immediately. So, it is very difficult to obtain the evolution of the composition of the cathode with time. The metal pedestal of the testing vacuum tube also prevents the imaging characteristics, the elemental distribution, and the structural analysis of the cathode surface. The analysis of the emission performance has been relying on theoretical speculation and experimental verification.

For high current density operations, when the electrons are emitted from the photocathode the inner areas of the photocathode become positively charged. Consequentially, only the most energetic electrons can overcome the resultant positive potential and be emitted. This effect prevents a high emission current. So, fine electronic contact needs to be designed near the emission areas to provide compensating electrons for the positively charged areas immediately. One practical conductive ring contact configuration is shown in Figure 5a. The photocathode and electronic contact are deposited on the same surface of the substrate. Owing to the sheet resistance of the alkali antimonide photocathode is about $1 \times 10^6 \Omega/\text{sq}$ to $1 \times 10^7 \Omega/\text{sq}$, a large potential difference between the inner area of the photocathode and the conductive ring is formed [21]. This large potential difference could cause a current increase from the adjacent areas of the emission area. It has been recorded that, when the photomultiplier tube is illuminated by an intense pulse laser with a repetitive frequency of kHz and a width of 10 nanoseconds, the time width of the current pulse will change to microsecond-level after 5 min. The broadening of the time width can be eliminated by improving the design of electronic contact. When the built-in electric field becomes sufficiently large, the electric breakdown could happen which will lead to a sudden increase in emission current. The electric breakdown will be very likely to cause an irreversible electrolytic decomposition of the cesium antimonide compound. This decomposition effect is easily recognizable by a change of the photocathode's color.

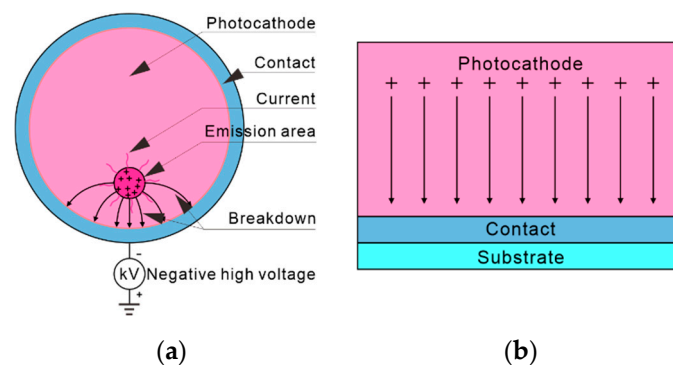


Figure 5. (a) Top view of the electric breakdown between positively charged photocathode emission area and electric contact which are on the same surface of the substrate; (b) side view of the built-in electric field between positively charged photocathode emission area and electrical contact designed in our experiments.

However, no color change is found during the experiments. The high current density operations can be well repeated over at least 20 times. Besides, the electric contact configuration used in the fabrication of this photocathode is different from the ring structure. In the ring contact configurations, the contact and photocathode are deposited on the same plane. In our layered fabrication structures, the aluminum contact film is coated on the substrate. Then, the photocathode is grown on the thin contact film. This structure can guarantee the electrons could be supplied to the emission areas. Even if there might be positively charged inside the photocathode, the built-in field is very low because the vertical-direction resistance of the photocathode is very low. The low potential difference between the inner area of the photocathode and the conductive film almost does not affect the emission performances.

Lastly, a possible reason for the current enhancement is the big roughness of the photocathode. This roughness causes a local distortion in the electric field. Previous research has shown that the roughness has a strong effect on emission emittance. The surface roughness is thought to limit the intrinsic emittance of alkali-antimonide cathodes to a 50% larger value than the thermal limit [22]. A simulation using VSim has studied the electron emission performance from a ridge period of 394 nm, ridge height of 194 nm, and a width of the ridge flat top of 79 nm. The results have shown that the quantum yield from the surface of the ridges is higher than from the flat surface [23]. This enhanced

field in the vacuum helps to lower the vacuum energy level and permit photoelectrons up cross the surface barriers, leading to an increase of the emission current [24]. It should be noted that the field enhancement in the vacuum can be the dominating reason for the increase of the emission current because it doesn't show any difference below 800 mW. Normally, roughness also causes reflection and scattering of the laser [25]. However, the thickness of the multi-alkali antimonide photocathode is below 100 nm, which makes the reflection and scattering contribute a little to the current enhancement.

For the flat cathode surface, the local electric field normal is perpendicular to the surface and the conductive thin metal film on the substrate, as shown in Figure 5b. The transverse field inside the cathode is zero. For the surface with a small roughness, the transverse fields are also weak. If the roughness of the cathode surface structure is big enough, the local electric field normal will differ greatly from the global normal, which is depicted in Figure 6. As we have discussed in Figure 5a, the transverse fields inner the photocathode emission areas could be strong enough to induce the current increase from its adjacent areas [26]. When the incident of the laser power is low, the emission current is also low, and the built-in electric field of the rough emission areas is too low to induce current from adjacent areas. When the emission current increases, the current density also increases, which causes a big field intensity. Therefore, the current will then be enhanced. However, in this case, the heat accumulation caused by the transverse sheet resistance cannot be ignored.

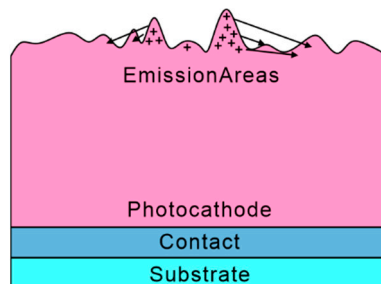


Figure 6. Side view built-in electric field between positively charged photocathode emission area and electric contact in our experiments.

To summarize, the current enhancement may be attributed to many effects. The enhancement in the built-in field caused by the roughness may be the dominant reason. The roughness can be attributed to the traditional photocathode growth procedures which we have already discussed at the beginning of this section. A previous ultrahigh vacuum atomic force microscope (UHV-AFM) study on bi-alkali antimonide photocathodes grown by the similar traditional procedures showed that the final rms surface roughness is about 25 nm over a 100 nm spatial period [27]. In recent years, the growth mechanism of sequentially grown bi-alkali antimonide K_2CsSb photocathodes has been studied by synchrotron X-ray techniques [28]. The randomly distributed roughness does cause problems to the uniformity problems and increase the emittance. If we look at the perspective of high quantum yield or emission current density, the roughness has advantages compared to the flat surface. In the future, controlled roughness technology needs to be studied by X-ray techniques. The current enhancement effect also inspired us to design and optimize the artificial rough structures of the substrate for practical applications [29].

The experimental evidence of high current density alkali antimonide photocathode has laid a very good foundation for us to further explore the possibility of continuously tunable CW THz sources. Electron emission from a surface with a controlled roughness can be utilized to improve the current density, though there must be a tradeoff with the energy spread and emittance of the initial electrons. It is foreseeable that the current density will be upgraded to an astonishing high value, for example beyond 10 A/cm^2 in CW mode. Similar to the Uni-traveling-carrier photodiode (UTC-PD) based THz emitter configuration, we could replace the solid-state photodiode with the photocathode emission THz vacuum photodiode. The vacuum photodiode enables bigger carrier mobility and allows more

carriers to transport. No electron diffusion problems exist. A detailed calculation shows that, for a photocathode with a conversion factor of 60 mA/W, the current is expected to be ~30 mA biased at 40 V by focusing the 500 mW laser into an area of 0.01 mm² [2]. This possible required area is far smaller than the testing emission area, which is circular with a diameter of 0.5 mm. When the impedance between the photoconductive vacuum tube and the high-gain antenna is matched, the THz radiation is expected to be beyond 20 mW, even if the conversion efficiency is 2%.

4. Conclusions

In conclusion, we have developed a high current density alkali antimonide photocathode and experimentally validated the repeatability, stability of the photocathode at different laser powers. The current enhancement effect has inspired us to further improve the current emission density through artificial rough substrate structures. Also, the linear zone of high current density emission can be used for THz photomixing modulation. The experimental evidence has laid a very good foundation for us to further explore the possibility of continuously tunable CW THz sources. The multi-alkali photocathode has the potential to provide high current density, small cross-section electron beams with long lifetimes, and lower cathode temperatures for practical use in THz vacuum devices.

Author Contributions: Writing—Original Draft Preparation, J.D., Writing—Review and editing, J.D., C.R. and X.X., methodology, J.D., X.X., H.L., data curation, J.D., validation, Y.D., and C.R., supervision, C.R., project administration, C.R. All authors have read and agreed to the published version of the manuscript.

Funding: This research was funded by the National Natural Science Foundation of China, grant number 61831001, and General Assembly Pre-Research Fund (6140862010116HK01001).

Conflicts of Interest: The authors declare no conflict of interest.

References

1. Dhillon, S.S.; Vitiello, M.S.; Linfield, E.H.; Davies, A.G.; Hoffmann, M.C.; Booske, J.; Paoloni, C.; Gensch, M.; Weightman, P.; Williams, G.P.; et al. The 2017 terahertz science and technology roadmap. *J. Phys. D Appl. Phys.* **2017**, *50*, 043001. [\[CrossRef\]](#)
2. Diamant, G.; Halahmi, E.; Kronik, L.; Levy, J.; Naaman, R.; Roulston, J. Integrated circuits based on nanoscale vacuum phototubes. *Appl. Phys. Lett.* **2008**, *92*, 262903. [\[CrossRef\]](#)
3. Dai, J.; Ruan, C.; Ding, Y.; Zhang, X. High Power Terahertz Source Based on Planar Antenna Integrated Vacuum Photodiode. In Proceedings of the 2019 Photonics & Electromagnetics Research Symposium—Spring (PIERS-Spring), Xiamen, China, 17–20 December 2019; pp. 3064–3067.
4. Levy, J. Electron Emission Device of High Current Density and High Operational Frequency. U.S. Patent No. 8143566, 27 March 2012.
5. Cultrera, L.; Lee, H.; Bazarov, I. Alkali antimonides photocathodes growth using pure metals evaporation from effusion cells. *J. Vac. Sci. Technol. Nanotechnol. Microelectron. Mater. Process. Meas. Phenom.* **2016**, *34*, 011202. [\[CrossRef\]](#)
6. Sommer, A.H. *Brief History of Photoemissive Materials*; Kaufmann, K.J., Ed.; International Society for Optics and Photonics: San Diego, CA, USA, 1993; p. 2.
7. Sommer, A.H. The element of luck in research—Photocathodes 1930 to 1980. *J. Vac. Sci. Technol. A Vac. Surf. Film.* **1983**, *1*, 119–124. [\[CrossRef\]](#)
8. Stovall, J. A Review of Radio-Frequency Photocathode Electron Sources. In Proceedings of the 1992 Linear Accelerator Conference (LINAC'92), Ottawa, ON, Canada, 24–28 August 1992; paper TU2-03. pp. 285–289.
9. Erjavec, B. Alkali metal vapour dynamics during Na₂KSb (Cs) photocathode growth. *Vacuum* **1992**, *43*, 1171–1175. [\[CrossRef\]](#)
10. Townsend, P.D. Photocathodes—Past performance and future potential. *Contemp. Phys.* **2003**, *44*, 17–34. [\[CrossRef\]](#)
11. Takahashi, A.; Nishizawa, M.; Inagaki, Y.; Koishi, M.; Kinoshita, K. New femtosecond streak camera with temporal resolution of 180 fs. In Proceedings of the SPIE, San Diego, CA, USA, 11 November 1994; Volume 2116, pp. 275–284.
12. Lee, C. High current density photoemissive electron source. *Appl. Phys. Lett.* **1984**, *44*, 565–566. [\[CrossRef\]](#)

13. Nishimori, N.; Nagai, R.; Sawamura, M.; Hajima, R. Development of a Multialkali Photocathode Dc Gun for a Smith-Purcell Terahertz Free-Electron Laser. *Particles* **2018**, *1*, 12. [\[CrossRef\]](#)
14. Erjavec, B. Alkali vapour pressure variations during Na₂KSb(Cs) photocathode synthesis. *Vacuum* **1994**, *45*, 617–622. [\[CrossRef\]](#)
15. Sommer, A.H. Stability of Photocathodes. *Appl. Opt.* **1973**, *12*, 90. [\[CrossRef\]](#) [\[PubMed\]](#)
16. Liu, Z.; Sun, Y.; Pianetta, P. High current density GaN/CsBr heterojunction photocathode with improved photoyield. *Appl. Phys. Lett.* **2007**, *4*. [\[CrossRef\]](#)
17. Ding, Z.; Gaowei, M.; Sinsheimer, J.; Xie, J.; Schubert, S.; Padmore, H.; Muller, E.; Smedley, J. In-situ synchrotron x-ray characterization of K₂CsSb photocathode grown by ternary co-evaporation. *J. Appl. Phys.* **2017**, *121*, 055305. [\[CrossRef\]](#)
18. Smedley, J.; Attenkofer, K.; Bhandari, H.; Ding, Z.; Frisch, H.J.; Gaowei, M.; Muller, E.M.; Padmore, H.A.; Schubert, S.G.; Sinsheimer, J.; et al. Sputter Growth of Alkali Antimonide Photocathodes: An in Operando Materials Analysis. In Proceedings of the International Particle Accelerator Conference, Richmond, VA, USA, 3–8 May 2015; pp. 1965–1967.
19. Natarajan, A.; Kalghatgi, A.T.; Bhat, B.M.; Satyam, M. Role of the cesium antimonide layer in the Na₂KSb/Cs₃Sb photocathode. *J. Appl. Phys.* **2001**, *90*, 6434–6439. [\[CrossRef\]](#)
20. Dai, J.; Ruan, C.; Xu, X.; Liu, H.; Ding, Y. High current density photocathode for CW terahertz photoconductive vacuum devices. *Vacuum* **2020**, *180*, 109587. [\[CrossRef\]](#)
21. Wright, A.G. *The Photomultiplier Handbook*; Oxford University Press: Oxford, UK, 2017; ISBN 0-19-252808-4.
22. Schubert, S.; Wong, J.; Feng, J.; Karkare, S.; Padmore, H.; Ruiz-Osés, M.; Smedley, J.; Muller, E.; Ding, Z.; Gaowei, M.; et al. Bi-alkali antimonide photocathode growth: An X-ray diffraction study. *J. Appl. Phys.* **2016**, *120*, 035303. [\[CrossRef\]](#)
23. Dimitrov, D.; Bell, G.; Ben-Zvi, I.; Karkare, S.; Padmore, H.; Smedley, J.; Smithe, D.; Zhou, C. 3D Modeling and Simulations of Electron Emission From Photocathodes With Controlled Rough Surfaces. In Proceedings of the 2nd North American Particle Accelerator Conference, København, Denmark, 14–19 May 2017; p. THPOA42.
24. Wieland, M.J.; Kampherbeek, B.J.; Addessi, P.; Kruit, P. Field emission photocathode array for multibeam electron lithography. *Microelectron. Eng.* **2001**, *57–58*, 155–161. [\[CrossRef\]](#)
25. Putnam, W.P.; Hobbs, R.G.; Keathley, P.D.; Berggren, K.K.; Kärtner, F.X. Optical-field-controlled photoemission from plasmonic nanoparticles. *Nat. Phys.* **2017**, *13*, 335–339. [\[CrossRef\]](#)
26. Dimitrov, D.; Bell, G.; Ben-Zvi, I.; Feng, J.; Karkare, S.; Padmore, H.; Smedley, J.; Smithe, D.; Veitzer, S. Modeling Cathode Roughness, Work Function, and Field Enhancement Effects on Electron Emission. In Proceedings of the 8th International Particle Accelerator Conference, Copenhagen, Denmark, 14–19 May 2017; p. THPAB066.
27. Schubert, S.; Ruiz-Osés, M.; Ben-Zvi, I.; Kamps, T.; Liang, X.; Muller, E.; Müller, K.; Padmore, H.; Rao, T.; Tong, X.; et al. Bi-alkali antimonide photocathodes for high brightness accelerators. *APL Mater.* **2013**, *1*, 032119. [\[CrossRef\]](#)
28. Ruiz-Osés, M.; Schubert, S.; Attenkofer, K.; Ben-Zvi, I.; Liang, X.; Muller, E.; Padmore, H.; Rao, T.; Vecchione, T.; Wong, J.; et al. Direct observation of bi-alkali antimonide photocathodes growth via *in operando* x-ray diffraction studies. *APL Mater.* **2014**, *2*, 121101. [\[CrossRef\]](#)
29. Hwang, S.-T.; Gil, B.; Yun, A.J.; Kim, J.; Kim, J.; Woo, H.; Park, K.; Park, B. Highly effective III-V solar cells by controlling the surface roughnesses. *Curr. Appl. Phys.* **2020**, *20*, 899–903. [\[CrossRef\]](#)

Publisher's Note: MDPI stays neutral with regard to jurisdictional claims in published maps and institutional affiliations.



© 2020 by the authors. Licensee MDPI, Basel, Switzerland. This article is an open access article distributed under the terms and conditions of the Creative Commons Attribution (CC BY) license (<http://creativecommons.org/licenses/by/4.0/>).